Published in final edited form as:
Arthritis Rheum. 2010 October ; 62(10): 2973–2983. doi:10.1002/art.27624.

Chondroprotective role of the osmotically-sensitive ion channel TRPV4: Age- and sex-dependent progression of osteoarthritis in *Trpv4* deficient mice

Andrea L. Clark, PhD[1], **Bartholomew J. Votta, MS**[3], **Sanjay Kumar, PhD**[3], **Wolfgang Liedtke, MD, PhD**[2], and **Farshid Guilak, PhD**[1]

[1] Department of Surgery, Duke University Medical Center, Durham, NC 27710

[2] Department of Medicine, Duke University Medical Center, Durham, NC 27710

[3] Department of Musculoskeletal Disease, GlaxoSmithKline Inc., King of Prussia, PA 19426

Abstract

Objectives—Mechanical loading significantly influences the physiology and pathology of articular cartilage, although the mechanisms of mechanical signal transduction are not fully understood. Transient receptor potential vanilloid 4 (TRPV4) is a calcium (Ca^{++}) permeable ion channel that is highly expressed by articular chondrocytes and can be gated by osmotic and mechanical stimuli. The goal of this study was to determine the role of *Trpv4* on the structure of the mouse knee joint and to determine whether *Trpv4*$^{-/-}$ mice exhibit altered Ca^{++} signaling in response to osmotic challenge.

Methods—Knee joints of *Trpv4*$^{-/-}$ mice were examined using histology and micro-computed tomography for osteoarthritic changes and bone structure at 4, 6, 9, and 12 months of age. Fluorescence imaging was used to quantify chondrocytic Ca^{++} signaling within intact femoral cartilage in response to osmotic stimuli.

Results—Deletion of *Trpv4* resulted in severe osteoarthritic changes, including cartilage fibrillation, eburnation, and loss of proteoglycans that were dependent on age and the male sex. Subchondral bone mass and calcified meniscal volume were greatly increased, again in male mice. Chondrocytes from *Trpv4*$^{+/+}$ mice demonstrated significant Ca^{++} responses to hypo-osmotic stress, but not hyper-osmotic stress. The response to hypo-osmotic stress or the TRPV4 agonist 4α-PDD was eliminated in *Trpv4*$^{-/-}$ mice.

Conclusions—Deletion of *Trpv4* leads to a lack of osmotically-induced Ca^{++} signaling in articular chondrocytes, accompanied by progressive, sex-dependent increases in bone density and osteoarthritic joint degeneration. These findings suggest a critical role for TRPV4-mediated Ca^{++} signaling in the maintenance of joint health and normal skeletal structure.

Keywords

transient receptor potential; arthritis; mechanical stress; articular cartilage; calcium channel; osmolarity; chondrocyte; ion channel

Corresponding author: Farshid Guilak, Ph.D., Orthopaedic Research Laboratories, 375 Medical Sciences Research Building, DUMC Box 3093, Duke University Medical Center, Durham, NC 27710, tel: (919) 684 2521, fax: (919) 681 8490.

INTRODUCTION

Articular cartilage, the avascular connective tissue that covers diarthrodial joint surfaces, provides a low-friction surface that supports and distributes joint loads. Cartilage comprises a hydrated extracellular matrix (ECM) of proteoglycans and collagen, as well as chondrocytes, the cells responsible for maintaining the ECM. Chondrocyte metabolic activity is regulated in part by physical factors such as mechanical loading (1–3). The transduction of biomechanical stress to an intracellular signal in cartilage represents a tissue-specific form of mechanotransduction that may involve a number of biophysical as well as biochemical events. Secondary to compression of the ECM, changes in the mechanical environment of cartilage can alter the pericellular osmolarity (4–6), potentially initiating various intracellular signal transduction pathways (7–13).

The cartilage ECM is inherently charged due to the large concentration of negatively charged proteoglycans, predominantly aggrecan. This fixed charge attracts free cations (e.g., Na^+, K^+, Ca^{++}), resulting in an increase in interstitial osmotic pressure that causes the tissue to retain water (14). Upon joint loading, water is exuded from the tissue and is reabsorbed when the tissue is no longer compressed (15). Thus, chondrocytes may experience acute as well as diurnal fluctuations in their osmotic environment as a result of normal joint loading, in addition to other mechanical stimuli such as cell deformation, fluid flow and fluid pressure (16–18). Chondrocytes respond to such osmotic fluctuations with the initiation of intracellular signaling cascades and acute volume change (9,10) followed by active volume regulation, which involves cytoskeletal F-actin restructuring as well as solute transport (8,10,19–22). In particular, osmotic stimulation elicits extracellular Ca^{++} influx, which is amplified by release from intracellular stores (9,10,12,23,24). The increase of intracellular Ca^{++} concentration may play a role in cell volume regulation, cell metabolism, and gene expression (25–27). Chondrocyte sensitivity to both mechanical and osmotic stress has been characterized at the cellular and tissue level, although the molecular mechanisms by which these cells sense external osmotic changes are not fully understood (2).

One novel potential candidate involved in chondrocyte mechano-osmotic signal transduction is the Ca^{++}-permeable, nonspecific cation channel Transient Receptor Potential Vanilloid 4 (TRPV4) (28–30). TRPV4 is a non-selective ion channel activated by numerous stimuli including hypo-osmolarity (31,32), volume increase, warmth, and certain phorbol esters including 4α-phorbol 12,13-didecanoate (4α-PDD) (33). *Trpv4*$^{-/-}$ mice have impaired responses to both hyper-and hypo-osmotic noxious stimuli, and demonstrate impaired osmotic sensing in the central nervous system with subsequently blunted behavioral and neuroendocrine homeostatic defense mechanisms (34). However, many aspects of the role of *Trpv4* in mammalian physiology are just emerging, such as *Trpv4*'s role in endothelial vascular functioning and in airways and lung (35,36). TRPV4 is expressed in many tissues, including the central nervous system, sensory neurons, kidney, upper and lower airways, salivary gland epithelia, endothelia, testis, and bone (37,38), yet is highly expressed in articular cartilage, where the channel protein is localized to the outer cell membrane including the chondrocyte's cilium (39–41).

Recently we demonstrated that in porcine chondrocytes, Ca^{++} signaling via TRPV4 regulates volume recovery following hypo-osmotic stimulation (41). Furthermore, the inhibition of chondrocyte signaling and volume regulation evoked by exposure to interleukin-1 (IL-1) was restored by activation of TRPV4 with 4α-PDD. The expression of TRPV4 in the chondrocyte membrane (and critically in the primary cilium), as well as the potent effects of 4α-PDD on volume regulation of chondrocytes, provides strong support for the concept that TRPV4 plays a major role in the Ca^{++} response of chondrocytes to compression-induced changes in their osmotic environment *in situ*. In addition to its role in

chondrocytes' response to osmotic challenge, TRPV4 has also been implicated as a regulator of chondrogenic differentiation, and TRPV4 shows similar expression patterns as the chondrogenic markers collagen II and aggrecan (40). Furthermore, TRPV4-mediated Ca^{++} influx evoked by 4α-PDD upregulates Sox9, an essential transcription factor for chondrocyte differentiation (40). Of interest, very recently, in humans, gain-of-function mutations of *Trpv4* have been linked to human brachyolmia, a skeletal deformation with short stature, scoliosis and vertebrate and long bone abnormalities, in addition to another skeletal disorder, Spondylometaphyseal Dysplasia (42,43). *Trpv4* is also expressed in both osteoblasts and osteoclasts, and TRPV4-mediated influx of Ca^{++} regulates the differentiation of osteoclasts (44). Deletion of *Trpv4* suppresses unloading-induced reduction in the levels of mineral apposition rate and bone formation rate (45). These data suggest a possible role for TRPV4 in cartilage skeletal development and maintenance. Whether morphology and function of diarthrodial joints depends on the *Trpv4* gene is currently not known.

In this study, we utilized *Trpv4* null mice to investigate the role of *Trpv4* in the *in vivo* development of spontaneous knee osteoarthritis as measured by histology and micro-computed tomography (μCT). Additionally, we measured Ca^{++} signaling in response to osmotic load in a novel *ex vivo* preparation using condylar chondrocytes within the intact native cartilage of femoral condyles of wild type and *Trpv4* deficient mice. *Ex vivo* condylar femoral chondrocytes from *Trpv4* null mice showed impaired Ca^{++} signaling in response to osmotic loading *in situ*. The absence of *Trpv4* resulted in severe, progressive osteoarthritic changes, particularly in male mice, that were accompanied by significant increases in ossification of joint tissues, suggesting a chondroprotective role for this channel possibly mediated by its Ca^{++} gating in response to hypotonicity.

METHODS

Generation of Trpv4 null (Trpv4$^{-/-}$) mice

All animal protocols were approved by the Duke University Institutional Animal Care and Use Committee (IACUC). *Trpv4* null mice were generated previously based on the zygotic *CRE-lox*-mediated excision of exon 12 of the *Trpv4* gene, which codes for the pore-loop and adjacent transmembrane domains (34). In this model, *Trpv4* is deleted from all tissues in the body. These mice were bred on the C57Bl6/J background strain past the tenth generation, and PCR-genotyped following established protocols based on isolation of genomic DNA from tail biopsies. Once genotyped, *Trpv4*$^{-/-}$ and *Trpv4*$^{+/+}$ were separated and maintained as separate colonies.

Immunolabeling for TRPV4

Immunohistochemistry was utilized to confirm the absence of the TRPV4 protein in chondrocytes from *Trpv4*$^{-/-}$ mice. The anti-TRPV4 polyclonal antibody (46) was used at 6.4 μg/ml. For immunodetection, we used a goat anti-mouse IgG Alexa Fluor 595 (Molecular Probes) diluted 1:750 in the same solution used with the primary antibody.

Micro-CT imaging

To examine changes in bone mineral density and structure, mouse limbs were imaged using three-dimensional μCT. Eight wild type and eight *Trpv4*$^{-/-}$ animals (four male and four female) were assigned to each of the 4, 6, 9 or 12 month age groups. The final 12 month time point was chosen after considering that C57Bl6/J mice have an 80% survival rate out to 24months and spontaneous knee osteoarthritis occurs in 39% of C57Bl6/J mice aged 12–17months (47). At each time point, six animals (n=3 male and n=3 female) were weighed and sacrificed. Skin was removed from the hindlimbs and the right legs dislocated at the hip and detached from the body. All leg muscles were left intact and the limbs stored submerged

in phosphate buffered saline (PBS) pH 7.4 in cryotubes at −80°C. Limbs were defrosted and then held at a physiological joint angle in a plastic cassette while submerged in 10% neutral buffered formalin overnight. Once fixed, each limb was held vertically in a foam mould and two limbs were carefully stacked on top of one another with their patellar tendons aligned vertically inside a formalin-filled scanning cylinder. The cylinder was then placed inside the μCT machine (microCT 40 Scanco Medical AG, Bassersdorf, Switzerland) for scanning. High intensity medium resolution (16μm) scans in the transverse plane were performed on each sample.

To distinguish calcified from soft tissues, an image intensity threshold was set and used for all images in the study using pilot limbs from wild type and *Trpv4*$^{-/-}$ mice. A hydroxylapatite (HA) phantom was used to scale the image intensity to bone density in mg HA/cm^3. Four regions of subchondral and trabecular bone were analyzed on each image; medial and lateral tibial plateaus and medial and lateral femoral condyles (Supplemental Figure S1). To examine differences in bone properties immediately below the cartilage layer (i.e. subchondral bone), this region was defined starting at the first transverse slice where the subchondral plate appeared in the center of the knee through to the twelfth slice either above or below, for femoral and tibial subchondral bone, respectively. To determine changes in trabecular bone properties, bone properties were determined in a region defined by the first transverse slice where trabecular bone appeared, through to the first slice above or below that where the growth plate was evident, for the femoral or tibial trabecular bone, respectively. As the knee menisci in mice are ossified structures, we evaluated the properties of the calcified regions of the menisci, including the anterior and posterior horns of the medial and lateral menisci (Supplemental Figure S1). All regions were outlined using a semi-automated contouring algorithm. Bone density and volume were evaluated for all contoured regions and apparent bone density was calculated for trabecular regions. Femoral and tibial subchondral bone thickness was measured from the sagittal section in the center of the medial and lateral load bearing regions of each hind limb. Three measurements across the section were made using image analysis software (Zeiss LSM Image browser) and the average was reported. Analysis of variance (ANOVA) with Tukey *post hoc* test was performed on all of the parametric morphological bone data.

Histology

After scanning, hindlimbs were dissected free of muscle leaving the knee capsule intact except for a small incision in the proximal patellar tendon. Hindlimbs were decalcified and then dehydrated in increasing concentrations of ethanol solution at room temperature. Samples were embedded in paraffin and histological sections (8μm thick) were cut throughout the entire knee width in the sagittal plane and stained with Hematoxylin, Fast Green and Safranin-O. Sections were graded for osteoarthritic changes by three blinded graders using a modified histological grading scheme (48). ANOVA with Tukey *post hoc* test was performed on the total histological grade data.

Fluorescence Imaging of Ca^{++} in Intact Femora

Specimen Preparation—Wild-type and *Trpv4*$^{-/-}$ mice (4–5 months old) were weighed, then euthanized. Immediately, hindlimbs were dislocated from the body and the femora isolated and cleaned of muscle, ligament and tendon tissue under a dissection microscope. The femora were frequently sprayed with media and fiber optic lighting was used to ensure that the femoral cartilage remained moist throughout. To confirm cell viability after dissection, preliminary studies were performed on isolated femora using a fluorescent viability assay (Invitrogen). After harvest, femora were submerged in medium (phenol-red free Dulbecco's Modified Eagles Medium (DMEM) (GibcoBRL, Grand Island, NY), 15mM Hepes (GibcoBRL), pH 7.4 at 37°C and 5% CO_2.

The femora were held between custom-built platens (Supplemental Figure S2) inside a heated perfusion chamber (Zeiss, Thornwood, NY) on an inverted confocal laser scanning microscope (LSM 510, Zeiss, Thornwood, NY). Femora were submerged in 2.5 ml of media with the femoral condylar cartilage resting on the coverslip. The temperature of the medium within the chamber was maintained at 37°C, measured by a temperature probe positioned next to the femora and varied less than 1°C throughout the 12 minutes of data collection.

Fluorescence Imaging—All femora were imaged on the day of isolation. Prior to imaging, the chondrocytes of the femora were loaded with two visible light fluorescent Ca^{++} indicators; Fura-Red AM (60 μM, decreases fluorescence with increased Ca^{++}) and Fluo-4 AM (16 μM, increases fluorescence with increased Ca^{++}) (Invitrogen-Molecular Probes, Eugene, OR) for 40 minutes. Transient changes in intracellular Ca^{++} concentration ($[Ca^{++}]_i$) were measured using an adaptation of a previously described ratiometric imaging technique (fluorescence of Fluo-4 divided by that of Fura Red) using a 40x objective lens (EC Plan Neofluar, Zeiss, numerical aperture 0.75) (49). This ratiometric approach serves to amplify the fluorescent signal and to correct for focal changes over the course of the test. The sample was excited using an argon ion laser (488 nm) and fluorescence emission was recorded at 505–550 nm (Fluo-4) and at greater than 650 nm (Fura-Red) (Figure 1). The pinholes of the confocal microscope were fully opened to allow collection of fluorescence from the entire cell. Nine scans were performed with the femora submerged in 300mOsm media before this media was withdrawn and replaced by vehicular control, anisosmotic media (200, 250, 300, 350 or 400mOsm) or 10μM 4α-PDD, in order to activate TRPV4 non-osmotically. Media osmolarity was altered by adding distilled water or sucrose to media and verified using a freezing point osmometer (Osmette A, Precision systems, Natick, MA). Sequential images (1024×1024, Figure 1A-D) were recorded at a scan rate of 0.28 Hz for 12 minutes to measure relative $[Ca^{++}]_i$.

Data Analysis—The ratiometric fluorescence was normalized to the average value over the first nine scans for each individual cell. A positive $[Ca^{++}]_i$ response was then defined as an increase in normalized ratiometric fluorescence greater than two standard deviations over the background noise, with both fluorescent indicators responding. The percentage of cells responding with single or multiple $[Ca^{++}]_i$ oscillations were examined. The magnitude, duration and time to each $[Ca^{++}]_i$ peak was measured together with the time between $[Ca^{++}]_i$ peaks and the rise time of each peak. The Chi squared test was applied to the non-parametric $[Ca^{++}]_i$ signaling data and ANOVA with Tukey *post hoc* test performed on the parametric data describing the $[Ca^{++}]_i$ peak characteristics.

RESULTS

Immunohistochemistry confirmed the absence of the TRPV4 protein in chondrocytes from *Trpv4*$^{-/-}$ mice (Supplemental Figure S3). The mice used in this study did not demonstrate any overt signs of altered gait or other signs of altered joint function during regular routine observations of the animals in their cages. Immediately after sacrifice, the knees showed no differences in laxity, stiffness or range of motion. On average male mice were heavier than female mice (male = 35.3±7.4g, female = 29.9±4.3g) and older mice heavier than younger mice (12 month female = 33.0±5.5g, 4 month female = 27.3±2.3g, 12 month male = 42.2±12.0g, 4 month male = 31.5±2.1g). There were no significant differences in body weight between wild-type and knockout mice (wild-type female = 29.5±4.1g, *Trpv4*$^{-/-}$ female = 30.3±4.5g, wild-type male = 35.4±9.4g, *Trpv4*$^{-/-}$ male = 35.2±4.3g).

μCT Imaging

Calcification and Ossification—MicroCT (μCT) imaging was performed to determine changes in bone architecture and bone mineral density with age (Figure 2). Enlargement of sesamoid bones and increased calcifications in the knee were qualitatively observed. These included the patellar tendon, both anterior and posterior to the patellar, and both sesamoid bones posterior to the femoral condyles (Figure 2). Increased calcification of the growth plate was also observed (Figure 2).

At 4, 6 and 9 months the calcified meniscal regions of both male and female wild type and *Trpv4*$^{-/-}$ mice had similar volume with the anterior regions being larger than posterior areas (Figure 3A and C). While menisci generally ossify with age in rodents, at 12 months there was a profound increase in calcified volume in all *Trpv4*$^{-/-}$ meniscal regions (Figure 2), with this effect being exacerbated in male compared to female mice (Figure 3A). On average, the volume of calcified meniscus was larger in *Trpv4*$^{-/-}$ mice compared to wild type in both anterior locations and in the posterior portion of the medial meniscus (Figure 3C). In addition, the density of these calcified portions of the menisci increased linearly with time and in a similar manner for wild type and *Trpv4*$^{-/-}$ mice (Figure 3B).

Subchondral Bone—*Trpv4*$^{-/-}$ male mice had larger subchondral bone volume compared to their wild type counterparts at 12 months (Figure 4A). This increase in volume could not be fully accounted for by an increase in subchondral thickness and thus includes expansion in the medial/lateral and anterior/posterior directions (Figure 2). In contrast, subchondral bone volume was similar at all time points for *Trpv4*$^{-/-}$ and wild type female mice (Figure 4A). On average, subchondral bone volume was larger in medial compared to lateral sites (except for the tibial plateau of *Trpv4*$^{-/-}$mice) and in femoral condyles compared to tibial plateaus (except for the lateral aspect of *Trpv4*$^{-/-}$ mice) (Figure 4C). Subchondral bone density increased in a linear fashion with time in both female and male *Trpv4*$^{-/-}$ and wild type mice (Figure 4B). Additionally, subchondral condylar regions were more dense than their plateau counterpart (data not shown).

Trabecular Bone—Trabecular bone density increased in a linear fashion with time in both female and male *Trpv4*$^{-/-}$and wild type mice (Figure 4D). Trabecular bone density was larger in wild type compared to *Trpv4*$^{-/-}$ mice in all regions except the medial tibial plateau and was larger in lateral condylar relative to tibial plateau regions for both wild type and *Trpv4*$^{-/-}$ mice (Figure 4E). For wild type and *Trpv4*$^{-/-}$ mice trabecular bone density of the tibial plateau was greater on the medial compared to the lateral side (Figure 4E). Trabecular bone apparent density was larger in all condylar regions relative to the plateau counterpart and medial compared to lateral equivalents except for the wild type femoral condyle (data not shown). There was no consistent relationship between trabecular bone apparent density and time in male or female *Trpv4*$^{-/-}$ or wild type mice (data not shown).

Histology

By qualitative and semi-quantitative histological measures, knockout mice showed age- and sex-related increases in joint abnormalities associated with osteoarthritic degeneration. At 12 months, male *Trpv4*$^{-/-}$ mice had larger histological scores than all other subjects (Figure 5A). These mice demonstrated severe end stage osteoarthritic pathology including complete cartilage erosion exposing subchondral bone on both femoral and tibial articulating surfaces (Figure 6). Furthermore, menisci were considerably enlarged throughout the joints. At 9 months, male *Trpv4*$^{-/-}$ mice had increased histological scores compared to their wild type equivalent, all 4 month-old mice, and female equivalent mice (Figure 5A). In complete contrast, there was no significant difference between female *Trpv4*$^{-/-}$ and wild type histological scores at any time point (Figure 5A). On average (pooled sexes), *Trpv4*$^{-/-}$ mice

had larger histological scores than wild type mice at femoral and tibial sites on both lateral and medial sides of the knee, although this effect was principally due to the differences in the male mice (Figure 5B). These scores were larger for both genotypes for the tibial compared to femoral articulating surfaces (Figure 5B).

Osmotically-induced Ca^{++} signaling in chondrocytes

The technique developed in this study allowed us measure changes in $[Ca^{++}]_i$ in chondrocytes that were maintained in their fully intact femoral condylar cartilage matrix environment. Experiments demonstrate a significant effect of hypo-osmolarity on $[Ca^{++}]_i$ in wild type but not *Trpv4*$^{-/-}$ mice (Figure 1E and 1F). In agreement, 4α-PDD evoked $[Ca^{++}]_i$ transients in wild type but not *Trpv4*$^{-/-}$ mice (Figure 1G). In contrast, hyper-osmolarity had no effect on $[Ca^{++}]_i$ in either wild type or *Trpv4*$^{-/-}$ preparations (Figure 1E and 1F).

The Ca^{++} responses in wild type mice were characteristically different for osmolarity compared to 4α-PDD stimuli. Peak magnitudes of $[Ca^{++}]_i$ were larger in magnitude and longer in duration with hypo-osmotic stimulation compared to 4α-PDD exposure (Supplemental Figure S4A and S4B). The latency between and rise time of $[Ca^{++}]_i$ peaks were both longer for osmotic compared to 4α-PDD stimulation (Supplemental Figure S4C and S4D). In contrast, time to peak was similar for hypo-osmotic and 4α-PDD exposure (Supplemental Figure S4E).

DISCUSSION

The findings of this study show that *Trpv4*$^{-/-}$ mice spontaneously develop osteoarthritis at a younger age and to a more severe extent than their wild-type controls. *Trpv4*$^{+/+}$ and *Trpv4*$^{-/-}$ mice were indistinguishable at 4 months of age by nearly every μCT and histological parameter measured, suggesting that TRPV4 expression is not necessary for skeletal development of the knee. However, significant deleterious changes were observed by 9 months, and by 12 months of age, *Trpv4*$^{-/-}$ mice exhibited erosions of the articular cartilage penetrating down through the subchondral bone. Furthermore, *Trpv4*$^{-/-}$ mice exhibited increased bone mass and overgrown, calcified menisci that completely surrounded the tibiofemoral compartments. Accompanying these changes was a loss of osmotically-activated Ca^{++} signaling in chondrocytes of *Trpv4*$^{-/-}$mice. These unexpected findings suggest that the mechanically and osmotically sensitive TRP channel, TRPV4, functions in a critical role in cartilage maintenance and “chondroprotection”, presumably via its role as a mediator of osmotically-activated Ca^{++} conductance in chondrocytes.

Another surprising result of our investigation was that the bony changes and osteoarthritic degeneration in *Trpv4*$^{-/-}$ mice was more pronounced in male mice as compared to females. This finding is in agreement with the majority of the literature examining spontaneous osteoarthritis in mice (50), as well as murine osteoarthritis models based on surgical intervention (51), or intraarticular injection (52). In all of these models, joint degeneration was found to be increased in male compared to female mice. Our present findings extend this concept to a genetically-encoded model of cartilage degeneration, namely the deletion of *Trpv4*. In contrast, the incidence and severity of osteoarthritis in humans is significantly higher in women compared to men, particularly after menopause (53–55). Little is currently known regarding the sex-specific expression of *Trpv4*. A recent study has shown that hyponatremia in humans is associated with a TRPV4 polymorphism but is present only in men (56). Furthermore, progesterone has been shown to regulate the expression of TRPV4 in human airway and mammary gland epithelial cells as well as in vascular smooth muscle cells (57). The exposure of these cells to progesterone decreased TRPV4 expression at both the gene and protein levels, thus diminishing 4α-PDD induced Ca^{++} signaling. The mechanisms responsible, be they gene- or channel-regulatory, for the sexual dimorphism of

the chondroprotective role of *Trpv4* remain to be determined, and future studies will address the obvious and pertinent questions, namely whether the *Trpv4* gene and/ or TPRV4 channel function is regulated by gonadal steroids.

In addition to cartilage and bone, *Trpv4* is present in many tissues throughout the body including the central nervous system, sensory neurons, kidney, upper and lower airways, salivary gland epithelia, endothelia and testis. The *Trpv4*$^{-/-}$ model utilized in this study is not tissue specific and therefore the changes observed in this study may also involve the loss of TRPV4 from other tissues. In future studies, conditional knockout models specific to the cartilage or bone may provide further insight into the specific role of TRPV4 in cartilage or bone.

Taken together with recently published reports, including our own on the role of TRPV4 in human and porcine articular chondrocytes, these studies reveal a critical role for the *Trpv4* gene in skeletal function (42–45). Our present analysis of mice with genetically-encoded deletion of *Trpv4* indicates that the knee shows progressive degeneration in the absence of *Trpv4* with first morphological signs at 9 months of age, and more severe cartilage loss at 1 year of age. Of note, this was observed with significant differences as compared to wildtype controls in male rather than in female mice.

In order to gather explanatory evidence at the level of the chondrocyte, we conducted Ca^{++} imaging in response to tonicity stimuli in chondrocytes in an *ex vivo* preparation using intact femoral condyles from wild type versus *Trpv4*$^{-/-}$ mice. In the absence of *Trpv4,* chondrocytes did not show an increased response to hypotonicity, or in other words, they were osmotically non-responsive. Under normal circumstances, the ability to respond to mechanical and/or osmotic stimuli constitutes a hallmark of chondrocyte physiology; thus, our basic insight of chondrocytes' non-responsiveness to hypotonicity in the absence of *Trpv4* could likely be a partial mechanistic explanation for the impaired homeostatic balance in the cartilage of *Trpv4* null mice. Lack of plasticity in response to hypo-osmotic stress translates to a lack of Ca^{++} influx into chondrocytes where it is needed in cellular volume homeostasis, namely to regulate increased cell volume. In this regard, our recent work with primary chondrocytes from porcine knee joints demonstrated that activation of TRPV4 is sufficient to rescue defective regulatory volume decrease evoked by interleukin-1 receptor (IL-1-R) signaling (41), a reductionist molecular model of the joint's inflammatory injury response in early osteoarthritis. Thus, TRPV4-mediated Ca^{++} influx into chondrocytes underlies a chondroprotective role. In other words, for genetically-encoded absence of *Trpv4*, over the animal's life-time an osmotic-sensing incompetent chondrocyte will likely be incompetent at maintaining tissue homeostasis as well, given the importance of mechano-osmotic signaling in the normal maintenance of cartilage physiology (2).

In addition, our Ca^{++} measurements demonstrate that stimulation of TRPV4 using either hypo-osmotic loading or the synthetic agent 4α–PDD led to contrasting characteristics in the resulting Ca^{++} transients. Calcium peaks were larger in magnitude and longer in duration in hypo-osmotic compared to 4α-PDD experiments. Further, the latency between and rise time of calcium peaks were both longer for osmotic compared to 4α-PDD stimulation. While these differences could perhaps be due to differences in the equivalent "dose" of hypo-osmotic stress as compared to 4α-PDD in activating TRPV4 in chondrocytes, these data rather suggest that different characteristics of the $[Ca^{++}]_i$ response depend on the TRPV4-specific stimulus modality. In regards to possible co-stimulated signaling pathways in response to hypotonicity in chondrocytes, our result of a complete absence of a $[Ca^{++}]_i$ response in *Trpv4* null mice points towards the predominant position of TRPV4 channels in such a signal transduction hierarchy, namely that TRPV4 is absolutely necessary for Ca^{++} to enter chondrocytes in response to hypotonicity.

In conclusion, we have shown that the genetically-encoded absence of *Trpv4* results in early and severe development of spontaneous osteoarthritis in male mice. This pathology appears throughout the joint and is first observed in articular cartilage at 9 months. At the cellular level, *Trpv4* is necessary for murine chondrocytes to transduce hypo-tonicity into Ca^{++} transients in intact femora. Together, these observations suggest a "chondroprotective" role for *Trpv4*, which plays a significant role in homeostasis and maintenance of articular cartilage, all of which in a sexually-dimorphic manner with male animals more susceptible to the arthritogenic sequelae of *Trpv4* deletion. Furthermore, an understanding of the role of TRPV4 and other ion channels on the response of chondrocytes to mechanical stimuli will provide new insights into the growth, development, and pathology of articular cartilage, as well as the potential for influencing cartilage regeneration in the context of tissue engineering.

Supplementary Material

Refer to Web version on PubMed Central for supplementary material.

Acknowledgments

The authors would like to thank Steve Johnson for exceptional help with all animal procedures, Greg Meyers for assistance with histological sectioning, staining and photography, Eric Mansfield for assistance with the Ca^{++} data analysis, Tim Griffin, Bridgette Furman and Holly Leddy for assistance with histological grading, and Sukhee Lee and Holly Leddy for TRPV4 immunohistochemistry. This study was supported by the Arthritis Foundation, GlaxoSmithKline, Inc., and NIH grants AR48182, AR48852, AR50245, and AG15768.

References

1. Griffin TM, Guilak F. The role of mechanical loading in the onset and progression of osteoarthritis. Exercise and Sport Sciences Reviews. 2005; 33(4):195–200. [PubMed: 16239837]
2. Guilak, F.; Hung, CT. Physical Regulation of Cartilage Metabolism. In: Mow, VC.; Huiskes, R., editors. Basic Orthopaedic Biomechanics and Mechanobiology. 3. Philadelphia: Lippincott Williams & Wilkins; 2004. p. 259-300.
3. Urban JPG, Hall AC, Gehl KA. Regulation of matrix synthesis rates by the ionic and osmotic environment of articular chondrocytes. Journal of Cellular Physiology. 1993; 154:262–70. [PubMed: 8425907]
4. Guilak F, Alexopoulos LG, Upton ML, Youn I, Choi JB, Cao L, et al. The pericellular matrix as a transducer of biomechanical and biochemical signals in articular cartilage. Ann N Y Acad Sci. 2006; 1068:498–512. [PubMed: 16831947]
5. Mow VC, Wang CC, Hung CT. The extracellular matrix, interstitial fluid and ions as a mechanical signal transducer in articular cartilage. Osteoarthritis Cartilage. 1999; 7(1):41–58. [PubMed: 10367014]
6. Alexopoulos LG, Setton LA, Guilak F. The biomechanical role of the chondrocyte pericellular matrix in articular cartilage. Acta Biomater. 2005; 1(3):317–25. [PubMed: 16701810]
7. Chao PG, Tang Z, Angelini E, West AC, Costa KD, Hung CT. Dynamic osmotic loading of chondrocytes using a novel microfluidic device. J Biomech. 2005; 38(6):1273–81. [PubMed: 15863112]
8. Chao PH, West AC, Hung CT. Chondrocyte intracellular calcium, cytoskeletal organization, and gene expression responses to dynamic osmotic loading. Am J Physiol Cell Physiol. 2006; 291(4):C718–25. [PubMed: 16928775]
9. Erickson GR, Alexopoulos LG, Guilak F. Hyper-osmotic stress induces volume change and calcium transients in chondrocytes by transmembrane, phospholipid, and G-protein pathways. J Biomech. 2001; 34(12):1527–35. [PubMed: 11716854]
10. Erickson GR, Northrup DL, Guilak F. Hypo-osmotic stress induces calcium-dependent actin reorganization in articular chondrocytes. Osteoarthritis Cartilage. 2003; 11(3):187–97. [PubMed: 12623290]

11. Hung CT, LeRoux MA, Palmer GD, Chao PH, Lo S, Valhmu WB. Disparate aggrecan gene expression in chondrocytes subjected to hypotonic and hypertonic loading in 2D and 3D culture. Biorheology. 2003; 40(1–3):61–72. [PubMed: 12454388]
12. Yellowley CE, Hancox JC, Donahue HJ. Effects of cell swelling on intracellular calcium and membrane currents in bovine articular chondrocytes. J Cell Biochem. 2002; 86(2):290–301. [PubMed: 12111998]
13. Sanchez JC, Wilkins RJ. Changes in intracellular calcium concentration in response to hypertonicity in bovine articular chondrocytes. Comp Biochem Physiol A Mol Integr Physiol. 2004; 137(1):173–82. [PubMed: 14720602]
14. Maroudas, A. Physicochemical properties of articular cartilage. In: MF, editor. Adult Articular Cartilage. Pitman Medical; Tunbridge Wells: 1979. p. 215-90.
15. Maroudas A, Wachtel E, Grushko G, Katz EP, Weinberg P. The effect of osmotic and mechanical pressures on water partitioning in articular cartilage. Biochimica et Biophysica Acta. 1991; 1073(2):285–94. [PubMed: 2009281]
16. Waterton JC, Solloway S, Foster JE, Keen MC, Gandy S, Middleton BJ, et al. Diurnal variation in the femoral articular cartilage of the knee in young adult humans. Magn Reson Med. 2000; 43(1): 126–32. [PubMed: 10642739]
17. Mow, VC.; Bachrach, NM.; Setton, LA.; Guilak, F. Stress, strain, pressure and flow-fields in articular cartilage and chondrocytes. In: Mow, VC.; Guilak, F.; Tran-Son-Tay, R.; Hochmuth, RM., editors. Cell Mechanics and Cellular Engineering. New York: Springer Verlag; 1994. p. 345-79.
18. Haider MA, Schugart RC, Setton LA, Guilak F. A mechano-chemical model for the passive swelling response of an isolated chondron under osmotic loading. Biomech Model Mechanobiol. 2006; 5(2–3):160–71. [PubMed: 16520959]
19. Kerrigan MJ, Hook CS, Qusous A, Hall AC. Regulatory volume increase (RVI) by in situ and isolated bovine articular chondrocytes. J Cell Physiol. 2006; 209(2):481–92. [PubMed: 16897756]
20. Borghetti P, Salda LD, De Angelis E, Maltarello MC, Petronini PG, Cabassi E, et al. Adaptive cellular response to osmotic stress in pig articular chondrocytes. Tissue & Cell. 1995; 27(2):173–83. [PubMed: 7778094]
21. Bush PG, Hall AC. The osmotic sensitivity of isolated and in situ bovine articular chondrocytes. Journal of Orthopaedic Research. 2001; 19:768–78. [PubMed: 11562120]
22. Bush PG, Hall AC. Regulatory volume decrease (RVD) by isolated and in situ bovine articular chondrocytes. J Cell Physiol. 2001; 187(3):304–14. [PubMed: 11319754]
23. Mobasheri A. Regulation of Na+, K+-ATPase density by the extracellular ionic and osmotic environment in bovine articular chondrocytes. Physiol Res. 1999; 48(6):509–12. [PubMed: 10783917]
24. Sanchez JC, Danks TA, Wilkins RJ. Mechanisms involved in the increase in intracellular calcium following hypotonic shock in bovine articular chondrocytes. Gen Physiol Biophys. 2003; 22(4): 487–500. [PubMed: 15113121]
25. McCarty NA, O'Neil RG. Calcium signaling in cell volume regulation. Physiol Rev. 1992; 72(4): 1037–61. [PubMed: 1332089]
26. Liu X, Bandyopadhyay BC, Nakamoto T, Singh B, Liedtke W, Melvin JE, et al. A role for AQP5 in activation of TRPV4 by hypotonicity: concerted involvement of AQP5 and TRPV4 in regulation of cell volume recovery. J Biol Chem. 2006; 281(22):15485–95. [PubMed: 16571723]
27. Hardingham GE, Bading H. Calcium as a versatile second messenger in the control of gene expression. Microsc Res Tech. 1999; 46(6):348–55. [PubMed: 10504212]
28. Liedtke W, Choe Y, Marti-Renom MA, Bell AM, Denis CS, Sali A, et al. Vanilloid receptor-related osmotically activated channel (VR-OAC), a candidate vertebrate osmoreceptor. Cell. 2000; 103(3):525–35. [PubMed: 11081638]
29. Strotmann R, Harteneck C, Nunnenmacher K, Schultz G, Plant TD. OTRPC4, a nonselective cation channel that confers sensitivity to extracellular osmolarity. Nat Cell Biol. 2000; 2(10):695–702. [PubMed: 11025659]
30. Nilius B, Voets T. TRP channels: a TR(I)P through a world of multifunctional cation channels. Pflugers Arch. 2005

31. Liedtke W. TRPV4 as osmosensor: a transgenic approach. Pflugers Arch. 2005
32. Liedtke WB. TRPV4 plays an evolutionary conserved role in the transduction of osmotic and mechanical stimuli in live animals. J Physiol. 2005
33. Nilius B, Watanabe H, Vriens J. The TRPV4 channel: structure-function relationship and promiscuous gating behaviour. Pflugers Arch. 2003
34. Liedtke W, Friedman JM. Abnormal osmotic regulation in trpv4−/− mice. Proc Natl Acad Sci U S A. 2003; 100(23):13698–703. [PubMed: 14581612]
35. Alvarez DF, King JA, Weber D, Addison E, Liedtke W, Townsley MI. Transient receptor potential vanilloid 4-mediated disruption of the alveolar septal barrier: a novel mechanism of acute lung injury. Circ Res. 2006; 99(9):988–95. [PubMed: 17008604]
36. Sidhaye VK, Guler AD, Schweitzer KS, D'Alessio F, Caterina MJ, King LS. Transient receptor potential vanilloid 4 regulates aquaporin-5 abundance under hypotonic conditions. Proc Natl Acad Sci U S A. 2006; 103(12):4747–52. [PubMed: 16537379]
37. Peng JB, Hediger MA. A family of calcium-permeable channels in the kidney: distinct roles in renal calcium handling. Curr Opin Nephrol Hypertens. 2002; 11(5):555–61. [PubMed: 12187321]
38. Guilak F, Leddy HA, Liedtke W. Transient receptor potential vanilloid 4: The sixth sense of the musculoskeletal system? Ann N Y Acad Sci. 2010; 1192(1):404–9. [PubMed: 20392266]
39. Mangos S, Liu Y, Drummond IA. Dynamic expression of the osmosensory channel trpv4 in multiple developing organs in zebrafish. Gene Expr Patterns. 2007; 7(4):480–4. [PubMed: 17161658]
40. Muramatsu S, Wakabayashi M, Ohno T, Amano K, Ooishi R, Sugahara T, et al. Functional gene screening system identified TRPV4 as a regulator of chondrogenic differentiation. J Biol Chem. 2007; 282(44):32158–67. [PubMed: 17804410]
41. Phan MN, Leddy HA, Votta BJ, Kumar S, Levy DS, Lipshutz DB, et al. Functional characterization of TRPV4 as an osmotically sensitive ion channel in articular chondrocytes. Arthritis & Rheumatism. 2009 in press.
42. Rock MJ, Prenen J, Funari VA, Funari TL, Merriman B, Nelson SF, et al. Gain-of-function mutations in TRPV4 cause autosomal dominant brachyolmia. Nat Genet. 2008; 40(8):999–1003. [PubMed: 18587396]
43. Krakow D, Vriens J, Camacho N, Luong P, Deixler H, Funari TL, et al. Mutations in the Gene Encoding the Calcium-Permeable Ion Channel TRPV4 Produce Spondylometaphyseal Dysplasia, Kozlowski Type and Metatropic Dysplasia. Am J Hum Genet. 2009
44. Masuyama R, Vriens J, Voets T, Karashima Y, Owsianik G, Vennekens R, et al. TRPV4-mediated calcium influx regulates terminal differentiation of osteoclasts. Cell Metab. 2008; 8(3):257–65. [PubMed: 18762026]
45. Mizoguchi F, Mizuno A, Hayata T, Nakashima K, Heller S, Ushida T, et al. Transient receptor potential vanilloid 4 deficiency suppresses unloading-induced bone loss. J Cell Physiol. 2008; 216(1):47–53. [PubMed: 18264976]
46. Lorenzo IM, Liedtke W, Sanderson MJ, Valverde MA. TRPV4 channel participates in receptor-operated calcium entry and ciliary beat frequency regulation in mouse airway epithelial cells. Proc Natl Acad Sci U S A. 2008; 105(34):12611–6. [PubMed: 18719094]
47. Jay GE Jr, Sokoloff L. Natural history of degenerative joint disease in small laboratory animals. II. Epiphyseal maturation and osteoarthritis of the knee of mice of inbred strains. AMA Arch Pathol. 1956; 62(2):129–35. [PubMed: 13354100]
48. Furman BD, Strand J, Hembree WC, Ward BD, Guilak F, Olson SA. Joint degeneration following closed intraarticular fracture in the mouse knee: a model of posttraumatic arthritis. J Orthop Res. 2007; 25(5):578–92. [PubMed: 17266145]
49. Lipp P, Niggli E. Ratiometric confocal Ca(2+)-measurements with visible wavelength indicators in isolated cardiac myocytes. Cell Calcium. 1993; 14(5):359–72. [PubMed: 8519060]
50. Silberberg M, Silberberg R. Osteoarthrosis and osteoporosis in senile mice. Gerontologia. 1962; 6:91–101. [PubMed: 13912809]
51. Ma HL, Blanchet TJ, Peluso D, Hopkins B, Morris EA, Glasson SS. Osteoarthritis severity is sex dependent in a surgical mouse model. Osteoarthritis Cartilage. 2007; 15(6):695–700. [PubMed: 17207643]

52. van Osch GJ, van der Kraan PM, Vitters EL, Blankevoort L, van den Berg WB. Induction of osteoarthritis by intra-articular injection of collagenase in mice. Strain and sex related differences. Osteoarthritis Cartilage. 1993; 1(3):171–7. [PubMed: 15449423]

53. Zhang Y, Jordan JM. Epidemiology of osteoarthritis. Rheum Dis Clin North Am. 2008; 34(3):515–29. [PubMed: 18687270]

54. Srikanth VK, Fryer JL, Zhai G, Winzenberg TM, Hosmer D, Jones G. A meta-analysis of sex differences prevalence, incidence and severity of osteoarthritis. Osteoarthritis Cartilage. 2005; 13(9):769–81. [PubMed: 15978850]

55. Lawrence RC, Felson DT, Helmick CG, Arnold LM, Choi H, Deyo RA, et al. Estimates of the prevalence of arthritis and other rheumatic conditions in the United States. Part II. Arthritis Rheum. 2008; 58(1):26–35. [PubMed: 18163497]

56. Tian W, Fu Y, Garcia-Elias A, Fernandez-Fernandez JM, Vicente R, Kramer PL, et al. A loss-of-function nonsynonymous polymorphism in the osmoregulatory TRPV4 gene is associated with human hyponatremia. Proc Natl Acad Sci U S A. 2009; 106(33):14034–9. [PubMed: 19666518]

57. Jung C, Fandos C, Lorenzo IM, Plata C, Fernandes J, Gene GG, et al. The progesterone receptor regulates the expression of TRPV4 channel. Pflugers Arch. 2009; 459(1):105–13. [PubMed: 19701771]

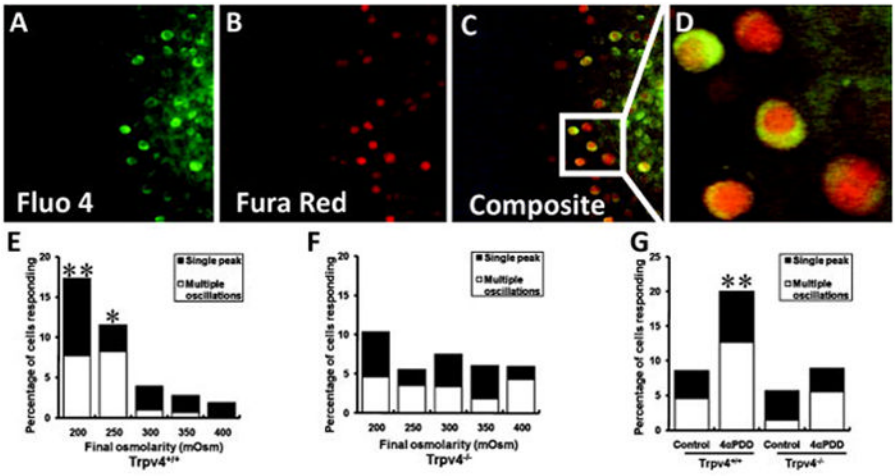

Figure 1.

Fluorescence imaging of $[Ca^{++}]_i$ showing different channels for (A) Fluo 4, (B) Fura Red, and (C) the composite ratio image. (D) A portion of the ratio image has been enlarged to demonstrate resolution. Lower panel shows the percentage of chondrocytes from (E) wild type and (F) *Trpv4*$^{-/-}$ femoral condyles responding with single or multiple calcium signals as a function of final osmolarity (starting osmolarity = 300mOsm for all cases) or (G) as a function of the presence or absence (control) of 4α-PDD. ******$p<0.01$ versus control; *****$p<0.05$ versus control, Chi-square analysis.

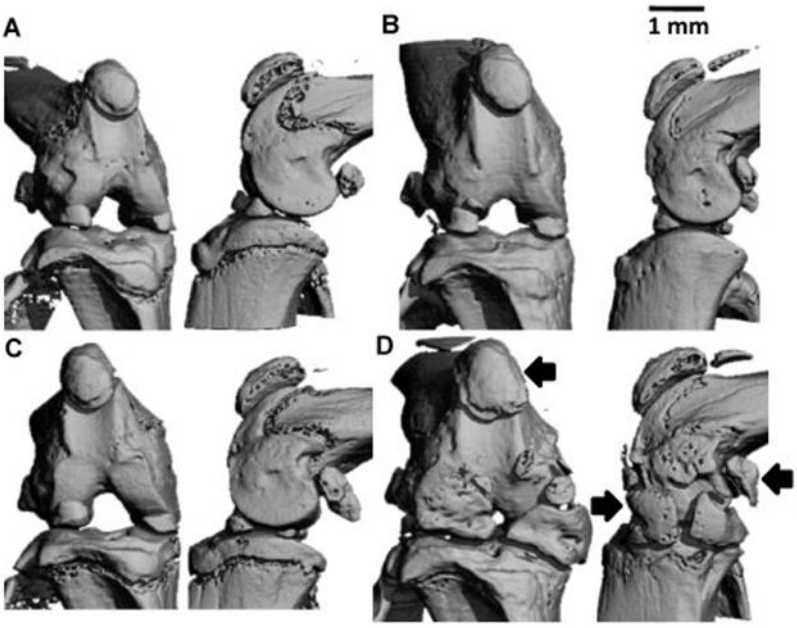

Figure 2.

Representative frontal (left) and sagittal (right) μCT views of the intact knee of male wildtype (A,B) and *Trpv4*$^{-/-}$ (C,D) mice. (A,C) 4 month old mice. (B,D) 12 month old mice. Scale bar = 1mm. Significant enlargement of the calcified regions of the menisci was observed, as well as that of the patella and condylar sesamoid bones (arrows), in *Trpv4*$^{-/-}$ mice at 12 months.

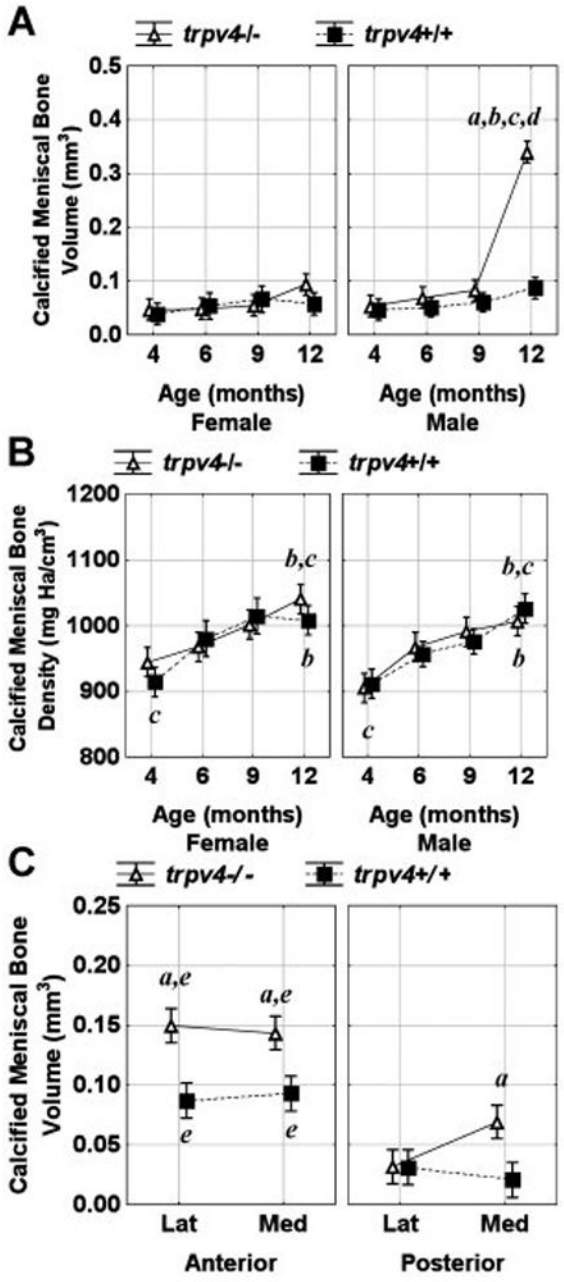

Figure 3.

Calcified meniscal bone volume (A) and density (B) as a function of age, sex and genotype. Calcified meniscal bone volume (C) as a function of site (lateral, medial), position (anterior, posterior) and genotype. Vertical bars represent 0.95 confidence intervals and significance is defined as $p<0.05$. [a]significant genotype difference between equivalent data points, [b]significant difference from all 4 month data points, [c]significant difference from 6 month equivalent data points, [d]significant difference from all other data points, and [e]significant difference between anterior and posterior equivalent data points.

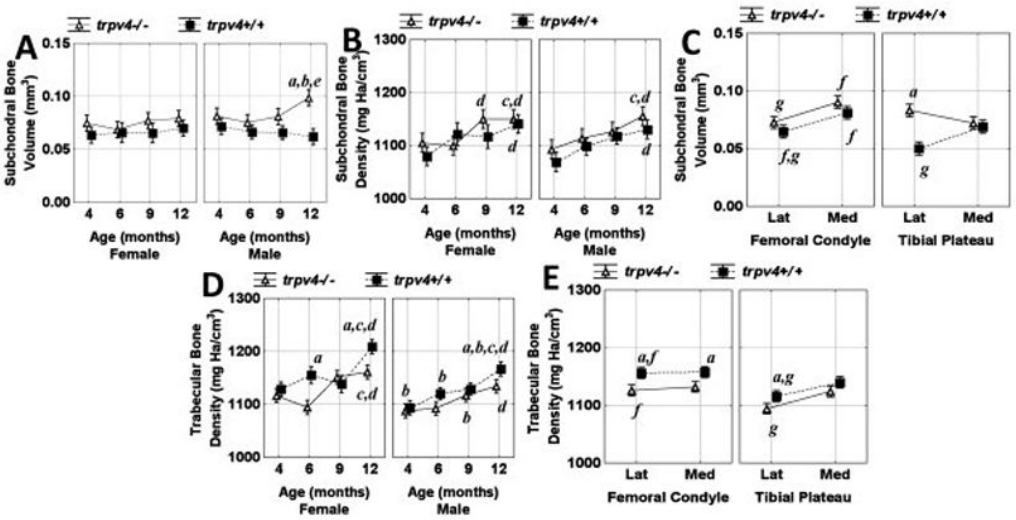

Figure 4.

Subchondral bone (A) volume and (B) density and (D) trabecular bone density as a function of age, sex, and genotype. Subchondral bone volume (C) and trabecular bone density (E) as a function of site: lateral (lat), medial (med), bone (femoral condyle/tibial plateau) and genotype. Vertical bars represent 0.95 confidence intervals and significance is defined as $p<0.05$. [a]significant genotype difference between equivalent data points, [b]significant sex difference between equivalent data points, [c]significant difference from all 4 month data points, [d]significant difference from 4 month equivalent data points, [e]significant difference from all other data points except 4 and 9 month equivalents, [f]significant difference between femoral and tibial equivalent data points and [g]significant difference between lateral and medial equivalent data points.

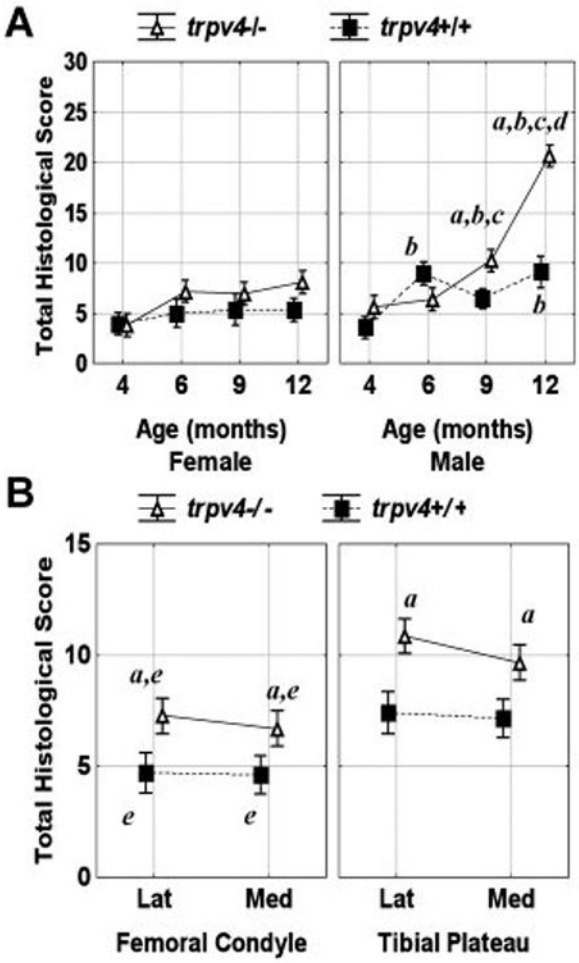

Figure 5.

Total histological score (A) as a function of age, sex and genotype, and (B) as a function of site: lateral (lat), medial (med), bone (femoral condyle/tibial plateau) and genotype. Vertical bars represent 0.95 confidence intervals and significance is defined as $p<0.05$. [a]significant genotype difference between equivalent data points, [b]significant sex difference between equivalent data points, [c]significant difference from all 4 month data points, [d]significant difference from all other data points, and [e]significant difference between femoral and tibial equivalent data points.

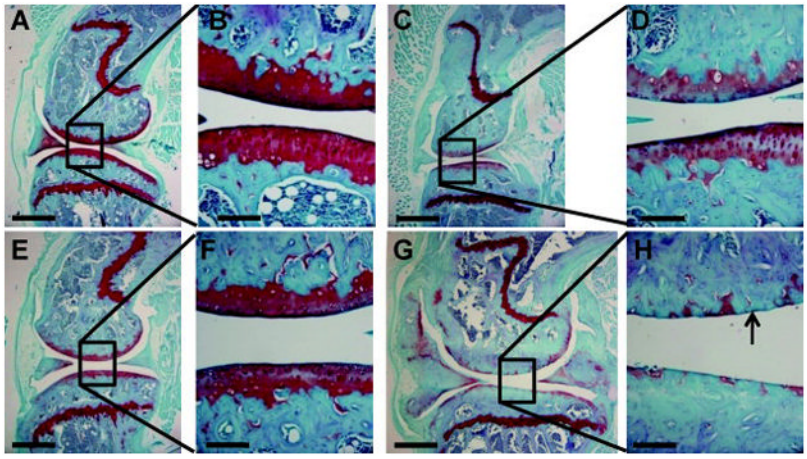

Figure 6.

Representative sagittal histology sections through the central region of the medial condyle of male wildtype (A-D) and *Trpv4*$^{-/-}$ (E-H) mice. (A,B,E,F) 4 month old mice. (C,D,G,H) 12 month old mice. Sections were stained with Hematoxylin, Fast Green and Safranin-O and imaged at 40× (A,C,E,G scale bar = 500μm) or 200× (B,D,F,H, scale bar = 100μm). Note the enlarged menisci, thickened subchondral bone and severe loss of articular cartilage (arrow) in *Trpv4*$^{-/-}$ mice at 12 months.